

# Water Segmentation on Elevated Noise SAR Imagery

Orlando Luscombe<sup>1</sup>

<sup>1</sup>Department of Electrical and Electronic Engineering at the University of Bristol

\*Corresponding author: [sv22482@bristol.ac.uk](mailto:sv22482@bristol.ac.uk)

## Abstract

This letter aims to understand the relationship between performance of water body mapping algorithms and the signal to noise ratio (SNR) of synthetic aperture RADAR (SAR) imagery. Through experimental analysis, we demonstrate when the SNR of an image is 10db and greater a segmentation F1-score of above 95% is achieved. This opens the possibility for lower SNR SAR systems in remote sensing applications. Finally, we discuss the experimental limitations regarding available datasets and direction of future research.

## Acronyms

|          |                               |
|----------|-------------------------------|
| SNR      | Signal To Noise Ratio         |
| F1-Score | (As seen in equation ??)      |
| SAR      | Synthetic Aperture Radar      |
| ERCS     | Effective Radar Cross Section |
| OT       | Otsu Thresholding             |
| Level-0  | ...                           |
| Level-1  | ...                           |

## 1. Introduction

Flood extent monitoring is an important task for earth observation satellites. Flooding events are often combined with cloud cover, therefore SAR's ability to make observations through cloud cover is critical for flood mapping.

The use of SAR cubesats is limited by power demands (as shown in Camps et al., 2023). Therefore, if power consumption (by RADAR transmission) can be reduced, whilst flood mapping cap-

abilities are retained, the possibility for constellations of cubesats with high revisit times and improved flood mapping abilities is realised. The revisit time of SAR satellites is important for flood map and prediction as demonstrated in Hostache et al., 2018. Artificially decreasing the SNR of RADAR images can be considered a simulation of lower RADAR transmission power. This is the approach used in this paper.

Current flood extent mapping methods fall into two main categories - thresholding and machine learning. An important phenomenon of flood detection is that bodies of water usually reflect RADAR signals away from their source whilst most in land areas typically return more of the signal. In thresholding methods the ERCS is grouped into higher and lower pixel value groups where areas with higher ERCS are assigned to water bodies and the lower ERCS to inland areas. The Otsu algorithm (OT)(see 1) is the basis for many of these methods such as in Tran et al., 2022.

Machine learning methods, unlike thresholding methods, do not directly group ERCS values. Instead these methods learn lower dimension representations of the input images to output a predicted flood map. In both methods ancillary data is important - ancillary data often includes DEM, hydro-logical maps and multispectral images. An advantage of machine learning methods and particularly convolutional neural networks is their ability to recognise artifacts similar to water

bodies, such as other low ERCS sources (elevation shadows, urban environments and large areas of sand) and use the context of the rest of the image to discern that they are not water bodies.

Figure 1

Otsu’s method determines the optimal threshold  $t^*$  that minimizes the within-class variance, defined as:

$$\sigma_w^2(t) = \omega_1(t)\sigma_1^2(t) + \omega_2(t)\sigma_2^2(t) \quad (1)$$

Minimising for:

$$t^* = \arg \min_t \sigma_w^2(t) \quad (2)$$

## 2. Methodology

The numerical experiments run in this letter use thresholding or machine learning methods to segment SAR images. First each method is tested with an example, in each example F1-score is used as the benchmark statistic (see equation ??). These test are performed using images from the mmfloods dataset<sup>1</sup>. Then an experiment focuses on a specific ROI (region of interest) using Level-0 data to test the impact of noise on each these methods.

$$F_1 = 2 \times \frac{TP}{(TP + FP) \times (TP + FN)} \quad (3)$$

where:

$TP$  = True Positives

$FP$  = False Positives

$FN$  = False Negatives

### 2.1 Thresholding Example

In this example only the VV polarisaed image is used (JUSTIFICATION same as test?). The raw image matrix  $I$  is pre-processed before OT. The information relevant to determine flooded and non-flooded regions is present in the darker

features of the image. Areas of high ERCS (artificial corner reflectors, metal structures and RF transmitters) are removed from the image by converting the image to a logarithmic scale and clipping the image output. As shown in the following equations.

$$I_{\log} = \log_{10}(I)$$

$$I_{\text{clipped}} = \min(\max(I_{\log}, 0), 0.005)$$

The extent to which an image must be clipped will change depending on the ROI however 0.005 was suitable for the majority of images in the mm-floods dataset. This clipping process acts as a initial threshold before OT. After clipping flooded areas can already be distinguished as seen in figure 3.

Figure 2

A: Post Otsu, B: Post CCA, C: Ground Truth



Next OT, then connected component analysis is performed - leaving the final prediction. Figure 2 shows the image post OT, post CCA (connected component analysis<sup>2</sup>) and the ground truth map.

Table 1: The confusion matrix (in-terms of pixel prediction):

|                 | Predicted Positive | Predicted Negative |
|-----------------|--------------------|--------------------|
| Actual Positive | 529299             | 14124              |
| Actual Negative | 7394               | 31519              |

The corresponding F1-Score for this classification is: 74.55%

Overall this method shows a good ability to segment water bodies from the input image.

<sup>1</sup><https://ieeexplore.ieee.org/document/9882096>

<sup>2</sup>OpenCv(connectedComponentsWithStats):[https://docs.opencv.org/3.4/d3/dc0/group\\_\\_imgproc\\_\\_shape.html](https://docs.opencv.org/3.4/d3/dc0/group__imgproc__shape.html)

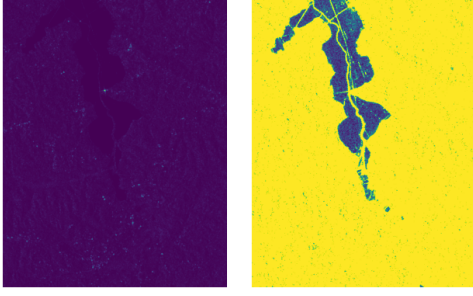


Figure 3: Comparison of pre-processed and raw SAR images (VV polarisation).

### 3. Increased Noise Experiment

To accurately simulate the effect of increased thermal noise of a SAR image, noise is added to the raw level-0 data. Then, to return to a level-1 image, range and azimuth compression is performed. ESA uses a more involved algorithm than just range and azimuth compression to convert from level-0 to level-1 images, but recreating this process is out of the scope of this letter (See this document<sup>3</sup> for more detail). This processing method limits the input images to strip-map mode acquisition. All level-0 data used in this experiment was downloaded from here<sup>4</sup>.

To simulate a lower SNR (higher noise floor) a random, normally distributed array of values are added to both the I and Q channels of the level-0 data. A range of SNR values are tested where the method shown in equation 4 is used.

To measure the performance of the segmentation the output is compared to the output of the segmentation when the input image has zero noise. Ideally one would compare the output to a ground truth as was possible when using the mmfloods data. A ground truth maps to match the level-0 data was found using google earth engine’s JRC Monthly Water History, v1.4 dataset.

<sup>3</sup><https://sentinel.esa.int/documents/247904/1877131/Sentinel-1-Level-1-Detailed-Algorithm-Definition>

<sup>4</sup><https://browser.dataspace.copernicus.eu/>

Method of Adding Noise to the Image Matrix:

$$\mu = \frac{1}{n} \sum_{i=1}^n |X_i|^2$$

$$P_{\text{noise}} = \frac{\mu}{\text{SNR}_{\text{Linear}}} \quad (4)$$

$$\mathbf{N} = \mathbf{N}_{\text{real}} + j\mathbf{N}_{\text{imag}}, \quad \sigma = \sqrt{\frac{P_{\text{noise}}}{2}}$$

$$\mathbf{Y} = \mathbf{X} + \mathbf{N}$$

Where  $\mathbf{Y}$  is the output image,  $\mathbf{X}$  is the input image and  $\mathbf{N}$  is the noise matrix.

However, difficulty aligning the level-0 data and ground truth map (potentially due to different coordinate basis) made this approach inaccurate. As we have shown the thresholding method can segment water bodies in section 2.1, we can compare the progressively noisy images to a segmented zero noise image to measure the change in segmentation accuracy. The results can be seen numerically in table ?? and visually in figures ?? and 5.

| SNR (dB) | F1-Score |
|----------|----------|
| -5       | Nan      |
| 0        | Nan      |
| 1.25     | 21.3979  |
| 2.5      | 53.2087  |
| 3.75     | 69.5172  |
| 5        | 83.117   |
| 10       | 97.191   |
| 20       | 98.918   |
| 30       | 99.386   |
| 40       | 99.093   |

Table 2: A table with SNR and F1-Score values.